Proceedings of the 2012
International Conference on
Computational and Mathematical
Methods in Science and Engineering
Murcia, Spain
July 2-5, 2012

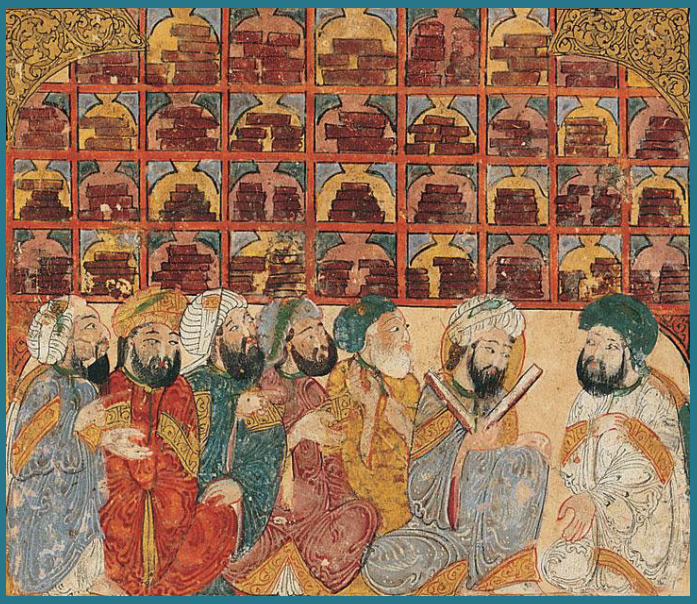

CMMSE

VOLUME I

Editor: J. Vigo-Aguiar

Associate Editors:
A.P. Buslaev, A. Cordero, M. Demiralp,
I. P. Hamilton, E. Jeannot, V.V. Kozlov,
M.T. Monteiro, J.J. Moreno, J.C. Reboredo,
P. Schwerdtfeger, N. Stollenwerk, J.R. Torregrosa,
E. Venturino, J. Whiteman

Proceedings of the 2012 International Conference on Computational and Mathematical Methods in Science and Engineering

La Manga, Murcia, Spain

July 2-5, 2012

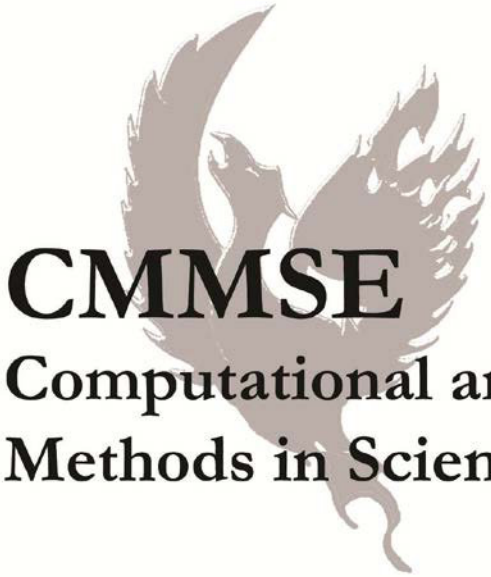

CMMSE

Computational and Mathematical Methods in Science and Engineering

Editor

J. Vigo-Aguiar

Associate Editors

A.P. Buslaev, A. Cordero, M. Demiralp,
I. P. Hamilton, E. Jeannot, V.V. Kozlov,
M.T. Monteiro, J.J. Moreno, J.C. Reboredo,
P. Schwerdtfeger, N. Stollenwerk, J.R. Torregrosa,
E. Venturino, J. Whiteman

Front cover: Arab anonymous painting
"The origin of Algebra"

ISBN 978-84-615-5392-1

Printed on acid-free paper
Volume I, II & III articles edited with LaTeX
Volume IV articles edited with Microsoft Word

Proceedings of the 12th International Conference
on Computational and Mathematical Methods
in Science and Engineering, CMMSE 2012
July, 2-5, 2012.

Quadratic B-splines on criss-cross triangulations for solving elliptic diffusion-type problems

Isabella Cravero[1], Catterina Dagnino[1] and Sara Remogna[1]

[1] *Department of Mathematics, University of Torino, via C. Alberto, 10 - 10123 Torino, Italy*

emails: isabella.cravero@unito.it, catterina.dagnino@unito.it, sara.remogna@unito.it

Abstract

In this paper we propose a method for the solution of elliptic diffusion-type problems based on bivariate quadratic B-splines on criss-cross triangulations. This technique considers the weak form of the differential problem and the Galerkin method to approximate the solution. As finite-dimensional space, we choose the space of quadratic splines on a criss-cross triangulation and we use its local basis both for the reconstruction of the physical domain and for the representation of the solution.

Beside the theoretical description, we provide some numerical examples.

Key words: elliptic diffusion-type problem, bivariate B-spline, criss-cross triangulation

MSC 2000: 65D07; 65N99

1 Introduction

Let $\Omega \subset \mathbb{R}^2$ be an open, bounded and Lipschitz domain, whose boundary $\partial\Omega$ is partitioned into two relatively open subsets, Γ_D and Γ_N, i.e. they satisfy $\emptyset \subseteq \Gamma_D, \Gamma_N \subseteq \partial\Omega$, $\partial\Omega = \bar{\Gamma}_D \cup \bar{\Gamma}_N$ and $\Gamma_D \cap \Gamma_N = \emptyset$. In this paper, we consider an elliptic diffusion-type problem with mixed boundary conditions

$$\begin{cases} -\nabla \cdot (K \nabla u) = f, & \text{in } \Omega, \\ \dfrac{\partial u}{\partial \mathbf{n}_K} = g_N, & \text{on } \Gamma_N, \quad \text{(Neumann conditions)} \\ u = g, & \text{on } \Gamma_D, \quad \text{(Dirichlet conditions)} \end{cases} \tag{1}$$

where $K \in \mathbb{R}^{2\times 2}$ is a symmetric positive definite matrix, $\mathbf{n}_K = K\mathbf{n}$ is the outward conormal vector on Γ_N, $f \in L^2(\Omega)$, $g_N \in L^2(\Gamma_N)$ and g is the trace on Γ_D of an $H^1(\Omega)$ function, i.e. $g \in H^{1/2}(\Gamma_D)$ (see [7]).

As noticed in [11], the diffusion type problem (1) arises in a variety of applications such as the temperature equation in heat conduction, the pressure equation in flow problems, and also mesh smoothing algorithms. If K is the identity matrix, (1) simplifies to Poisson's problem.

A standard method to find the approximate solution of (1) is the Finite Element Method (see e.g. [7]) and, over the last years, the Isogeometric Analysis (IGA) (see e.g. [5]). Usually IGA is based on NURBS defined by B-splines of tensor product type (see e.g. [1, 4]) or, recently, on quadratic Powell-Sabin splines (see [10]). In this paper we propose an IGA approach for (1), based on bivariate quadratic B-splines on criss-cross triangulations. As remarked in [13], functions having total degree are preferable, in some cases, to tensor product ones that may have some inflection points, due to their higher coordinate degree.

The paper is organized as follows. In Section 2 we recall definitions and properties of bivariate quadratic B-splines on criss-cross triangulations and, in Section 3, we use them for the solution of (1). Finally, in Section 4 we give some numerical examples.

2 Quadratic B-splines on criss-cross triangulations

In order to have a self-contained presentation, in this section we briefly recall definitions and properties of unequally smooth bivariate quadratic B-splines on criss-cross triangulations (for details see [3, 13] and the references therein).

Let $\Omega_0 = \{(s,t) \mid 0 \le s,t \le 1\}$ and m, n be positive integers. We consider the sets $\bar{\xi} = (\xi_i)_{i=0}^{m+1}$ and $\bar{\eta} = (\eta_j)_{j=0}^{n+1}$, with $0 = \xi_0 < \xi_1 < \ldots < \xi_{m+1} = 1$, $0 = \eta_0 < \eta_1 < \ldots < \eta_{n+1} = 1$, that partition Ω_0 into $(m+1)(n+1)$ rectangular cells. By drawing both diagonals for each cell, we obtain a non-uniform criss-cross triangulation $\mathcal{T}_{mn}$, made of $4(m+1)(n+1)$ triangular cells. Let $\mathcal{S}_2^{(\bar{\mu}^\xi,\bar{\mu}^\eta)}(\mathcal{T}_{mn})$ be the space of bivariate quadratic piecewise polynomials on $\mathcal{T}_{mn}$, where

$$\bar{\mu}^\xi = (\mu_i^\xi)_{i=1}^m \quad \text{and} \quad \bar{\mu}^\eta = (\mu_j^\eta)_{j=1}^n \tag{2}$$

are vectors whose elements can be either 1 or 0 and denote the smoothness C^1, C^0, respectively, across the inner grid lines $s - \xi_i = 0$, $i = 1,\ldots,m$ and $t - \eta_j = 0$, $j = 1,\ldots,n$, while the smoothness across all oblique mesh segments[1] is C^1.

Let L_s^0 and L_t^0 be the number of grid lines $s - \xi_i = 0$, $i = 1,\ldots,m$ and $t - \eta_j = 0$, $j = 1,\ldots,n$, respectively, across which we want $S \in \mathcal{S}_2^{(\bar{\mu}^\xi,\bar{\mu}^\eta)}(\mathcal{T}_{mn})$ has C^0 smoothness. We

[1] According to [12], we call *mesh segments* the line segments that form the boundary of each triangular cell of $\mathcal{T}_{mn}$.

 ISBN:978-84-615-5392-1

recall that (see [3])

$$\dim \mathcal{S}_2^{(\bar{\mu}^\xi,\bar{\mu}^\eta)}(\mathcal{T}_{mn}) = mn + 3m + 3n + 8 + (n+2)L_s^0 + (m+2)L_t^0.$$

We remark that, if $S \in \mathcal{S}_2^{(\bar{\mu}^\xi,\bar{\mu}^\eta)}(\mathcal{T}_{mn})$ is globally C^1 (i.e. $L_s^0 = L_t^0 = 0$), we obtain the well-known dimension of $\mathcal{S}_2^1(\mathcal{T}_{mn})$ (see [12]).

Furthermore, we can provide a local basis for $\mathcal{S}_2^{(\bar{\mu}^\xi,\bar{\mu}^\eta)}(\mathcal{T}_{mn})$ (see [3]). In order to do it, we set $M = 3 + \sum_{i=1}^m (2 - \mu_i^\xi)$ and $N = 3 + \sum_{j=1}^n (2 - \mu_j^\eta)$, where μ_i^ξ, μ_j^η are defined as in (2). Let $\bar{s} = (s_i)_{i=-2}^M$, $\bar{t} = (t_j)_{j=-2}^N$ be the nondecreasing sequences of knots, obtained from $\bar{\xi}$ and $\bar{\eta}$ by the following two requirements:

(i) $s_{-2} = s_{-1} = s_0 = \xi_0 = 0, \qquad s_{M-2} = s_{M-1} = s_M = \xi_{m+1} = 1,$
$t_{-2} = t_{-1} = t_0 = \eta_0 = 0, \qquad t_{N-2} = t_{N-1} = t_N = \eta_{n+1} = 1;$

(ii) for $i = 1, \ldots, m$, the number ξ_i occurs exactly $2 - \mu_i^\xi$ times in $\bar{s}$ and for $j = 1, \ldots, n$, the number η_j occurs exactly $2 - \mu_j^\eta$ times in $\bar{t}$.

For the above sequences $\bar{s}$ and $\bar{t}$, we consider the following set of functions belonging to $\mathcal{S}_2^{(\bar{\mu}^\xi,\bar{\mu}^\eta)}(\mathcal{T}_{mn})$

$$\mathcal{B} = \{B_{ij}(s,t)\}_{(i,j)\in\mathcal{K}_{MN}}, \tag{3}$$

where $\mathcal{K}_{MN} = \{(i,j) : 0 \le i \le M-1, 0 \le j \le N-1\}$. If both/either $\bar{s}$ and/or $\bar{t}$ have/has double knots, then the B_{ij} smoothness will change and the support will change as well. Moreover, the B_{ij}'s have a local support, are non negative and form a partition of unity. In $\mathcal{B}$ we find different types of spline functions. There are $\rho = 2M + 2N - 4$ unequally smooth functions, that we call *boundary B-splines*, whose restrictions to $\partial\Omega_0$ are univariate quadratic B-splines. The remaining $MN - \rho$ functions, called *inner B-splines*, are such that their restrictions to $\partial\Omega_0$ are equal to zero. The supports and the BB-coefficients of such B-splines are reported in [2].

Since $\sharp\mathcal{B} > \dim \mathcal{S}_2^{(\bar{\mu}^\xi,\bar{\mu}^\eta)}$, the functions belonging to $\mathcal{B}$ are linearly dependent. Let:

(i) $\{\Omega_{0,r}\}_{r=1}^\gamma$ be a partition of Ω_0 into rectangular subdomains, generated by the grid lines with associated C^0 smoothness, with $\gamma = (L_s^0 + 1)(L_t^0 + 1)$;

(ii) $\mathcal{B}$ be defined as in (3);

(iii) $\mathcal{B}_1 \subset \mathcal{B}$ be the set of inner B-splines with C^1 smoothness everywhere or with C^0 smoothness only on the boundary of their support;

(iv) $\{\mathcal{B}^{(r)}\}_{r=1}^\gamma$ be a partition of $\mathcal{B}_1$, where each $\mathcal{B}^{(r)}$ contains B-splines with support in $\Omega_{0,r}$.

 ISBN:978-84-615-5392-1

Then, we can prove that a B-spline basis for $\mathcal{S}_2^{(\bar{\mu}^\xi,\bar{\mu}^\eta)}(\mathcal{T}_{mn})$ can be extracted from $\mathcal{B}$, by removing γ B-splines, one in each $\mathcal{B}^{(r)},\ r=1,\dots,\gamma$ (see [3]). We denote the corresponding set of indices of the B-spline basis by $\bar{\mathcal{K}}_{MN}$.

We remark that, if $\mathcal{S}_2^{(\bar{\mu}^\xi,\bar{\mu}^\eta)}(\mathcal{T}_{mn}) \equiv \mathcal{S}_2^1(\mathcal{T}_{mn})$, then, from [9] and standard arguments in approximation theory, for all $H \in C^3(\Omega_0)$ there exist a constant $C>0$ such that

$$\inf_{S\in\mathcal{S}_2^1(\mathcal{T}_{mn})} \|H-S\|_\infty \leq Ch^3 \max\left\{\|D^{\alpha_1,\alpha_2}f\|_\infty : \alpha_1+\alpha_2=3\right\}$$

where $h=\max\{diam(T) \mid T \text{ is a triangle of } \mathcal{T}_{mn}\}$.

Since we are interested in the application of bivariate quadratic B-splines to the solution of (1), given the physical domain $\Omega \subset \mathbb{R}^2$, defined as in Section 1, we assume that such a domain can be exactly described through a parametrization of the form

$$\mathbf{G}:\Omega_0 \to \bar{\Omega}, \qquad \mathbf{G}(s,t)=\begin{pmatrix} x \\ y \end{pmatrix} \tag{4}$$

expressed as quadratic B-spline surface

$$\mathbf{G}(s,t)=\sum_{(i,j)\in\mathcal{K}_{MN}} \mathbf{P}_{ij}\ B_{ij}(s,t), \tag{5}$$

where $\{\mathbf{P}_{ij}\}_{(i,j)\in\mathcal{K}_{MN}}$ is a bidirectional net of control points, with $\mathbf{P}_{ij}\in\mathbb{R}^2$. We assume $p_{ij}=(s_i^p,t_j^p)\in\Omega_0$ as the pre-image of $\mathbf{P}_{ij}$, with

$$s_i^p=\frac{s_{i-1}+s_i}{2}, \qquad t_j^p=\frac{t_{j-1}+t_j}{2}. \tag{6}$$

We remark that, in order to construct the surface, it is not necessary to work with the basis, but we can use all the functions in the spanning set $\mathcal{B}$. In this case, the surface (5) has both the convex hull property and the affine transformation invariance one.

The proposed parametrization (5) is able to exactly reproduce domains whose boundary is made of linear and parabolic sections. In order to do it, the control points are obtained either by interpolation or quasi-interpolation spline operators (see [9, 12]).

Since the domains of interest in engineering problems are often described by conic sections, a possible extension of the current paper is to consider bivariate NURBS based on the B-splines here presented and we are working on it.

3 The Galerkin method based on bivariate quadratic B-splines

In this section, we consider an elliptic diffusion-type problem (1), where, for the sake of simplicity, we first assume homogeneous Dirichlet conditions, i.e. $g\equiv 0$. The weak formulation of (1) (see e.g. [5, 7]) is to find $u\in\mathbb{V}$ such that

$$a(u,v)=F(v), \quad \forall v\in\mathbb{V}, \tag{7}$$

 ISBN:978-84-615-5392-1

where:

- $\mathbb{V} = \{v \in H^1(\Omega) : v = 0 \text{ on } \Gamma_D\}$ is the space of functions with vanishing trace on Γ_D;
- $a : \mathbb{V} \times \mathbb{V} \to \mathbb{R}$ is the bilinear form given by $a(u, v) = \int_\Omega (K\nabla u) \cdot \nabla v \; d\Omega$;
- $F : \mathbb{V} \to \mathbb{R}$ is the linear functional given by $F(v) = \int_\Omega fv \; d\Omega + \int_{\Gamma_N} g_N v \; d\Gamma_N$.

In the Galerkin method to approximate the solution of (7), we replace the infinite dimensional space $\mathbb{V}$ by a finite-dimensional subspace $\mathbb{V}_h \subset \mathbb{V}$, with the subscript h indicating the relation to a spatial grid. Then, the discretized problem is to find $u_h \in \mathbb{V}_h$ such that

$$a(u_h, v_h) = F(v_h), \quad \forall v_h \in \mathbb{V}_h, \tag{8}$$

where $a(u_h, v_h) = \int_\Omega (K\nabla u_h) \cdot \nabla v_h \; d\Omega$ and $F(v_h) = \int_\Omega f v_h \; d\Omega + \int_{\Gamma_N} g_N v_h \; d\Gamma_N$.

Since, in (4), we have introduced the parametrization $\mathbf{G}$, we consider

$$\mathbb{V}_h = \left\{ v_h \in \mathbb{V} : \; v_h = v_{0,h} \circ \mathbf{G}^{-1}, \; v_{0,h} \in \mathbb{V}_{0,h} \right\},$$

where $\mathbb{V}_{0,h}$ is the discrete space in the parametric domain, that has to be chosen. In this paper, we consider $\mathbb{V}_{0,h}$ as an opportune subspace of $\mathcal{S}_2^{(\bar{\mu}^\xi, \bar{\mu}^\eta)}(\mathcal{T}_{mn})$.

Let N_h be the dimension of the spaces $\mathbb{V}_h$ and $\mathbb{V}_{0,h}$, and let $\{\Phi_l\}_{l=1}^{N_h}$ be a basis for $\mathbb{V}_{0,h}$. Then, we can define a basis for $\mathbb{V}_h$ as $\left\{\varphi_l = \Phi_l \circ \mathbf{G}^{-1}\right\}_{l=1}^{N_h}$ and the approximate solution u_h is given by

$$u_h = \sum_{l=1}^{N_h} q_l \varphi_l = \sum_{l=1}^{N_h} q_l (\Phi_l \circ \mathbf{G}^{-1}),$$

with unknown coefficients $q_l \in \mathbb{R}$. Therefore, (8) gives rise to

$$\sum_{l=1}^{N_h} q_l a(\varphi_l, \varphi_i) = F(\varphi_i), \quad i = 1, \ldots, N_h, \tag{9}$$

that is equivalent to the linear system $A\mathbf{q} = \mathbf{f}$, where

- $A \in \mathbb{R}^{N_h \times N_h}$ is the stiffness matrix with elements

$$A_{il} = a(\varphi_l, \varphi_i) = \int_\Omega (K\nabla\varphi_l) \cdot \nabla\varphi_i \; d\Omega, \qquad i, l = 1, \ldots, N_h; \tag{10}$$

- $\mathbf{f} \in \mathbb{R}^{N_h}$ is the vector with components

$$\mathbf{f}_i = F(\varphi_i) = \int_\Omega f\varphi_i \; d\Omega + \int_{\Gamma_N} g_N \varphi_i \; d\Gamma_N = \mathbf{f}_i^{(1)} + \mathbf{f}_i^{(2)}, \qquad i = 1, \ldots, N_h; \tag{11}$$

 ISBN:978-84-615-5392-1

- $\mathbf{q} \in \mathbb{R}^{N_h}$ is the vector of unknown coefficients q_l, $l = 1, \ldots, N_h$.

Here, we assume that the parametrization $\mathbf{G}$ is given by (5) and consequently, we get $\mathbb{V}_h \subset \text{span}\left\{B_{ij} \circ \mathbf{G}^{-1}\right\}_{(i,j)\in\bar{\mathcal{K}}_{MN}}$. Note that the boundary condition $u = 0$ has also to be considered and for this reason we write $\mathbb{V}_h$ as a subset of the span. Then, the approximate solution is obtained taking into account the homogeneous boundary conditions.

The integrals A_{il} in (10) and $\mathbf{f}_i^{(1)}$ in (11), can be transformed as follows

$$\begin{aligned} A_{il} &= \int_{\Omega_0} \left(K\left[J^{-T}\nabla\Phi_l\right]\right) \cdot \left[J^{-T}\nabla\Phi_i\right] |\text{det}J| \; d\Omega_0, \quad i,l = 1,\ldots,N_h, \\ \mathbf{f}_i^{(1)} &= \int_{\Omega_0} (f \circ \mathbf{G})\, \Phi_i \, |\text{det}J| \; d\Omega_0, \quad i = 1,\ldots,N_h, \end{aligned} \tag{12}$$

with J the Jacobian matrix of the parametrization $\mathbf{G}$ given in (4) and (5)

$$J = J(s,t) = \begin{bmatrix} \frac{\partial x(s,t)}{\partial s} & \frac{\partial x(s,t)}{\partial t} \\ \frac{\partial y(s,t)}{\partial s} & \frac{\partial y(s,t)}{\partial t} \end{bmatrix}.$$

To evaluate the boundary term $\mathbf{f}_i^{(2)}$ in (11), we first define the mapping $\mathbf{G}_b : I := (0,1) \to \Gamma_N$ as the restriction of $\mathbf{G}$ to the subset of $\partial\Omega_0$ mapped into Γ_N, assuming that each side of Ω_0 is completely mapped into Γ_N or Γ_D. Then,

$$\mathbf{f}_i^{(2)} = \int_I (g_N \circ \mathbf{G}_b)\, \Phi_i \left|\mathbf{G}_b'\right| \; dI. \tag{13}$$

In order to compute $\nabla\Phi_i$, $i = 1,\ldots,N_h$, and J in (12), we obtain the values of the B-spline derivatives by means of their BB-coefficients (see [8]).

For the evaluation of the integrals in (12), we use a composite Gaussian Quadrature on triangular domains (see [6]) implemented by the Matlab function `triquad` (see [14]). Given in input the integer p and the vertices of a triangle of $\mathcal{T}_{mn}$, this procedure computes the p^2 nodes and the corresponding weights of the rule, whose precision degree is $2p-1$. In the numerical tests proposed in Section 4, we use $p = 2$. When $\mathbf{G}$ is the identity map (i.e. $\bar{\Omega} \equiv \Omega_0$) then, in (12),

$$A_{il} = \int_{\Omega_0} (K\nabla\Phi_l) \cdot \nabla\Phi_i \; d\Omega_0, \quad i,l = 1,\ldots,N_h,$$

and it is exactly computed, since in each triangle of $\mathcal{T}_{mn}$ the integrand function is a bivariate quadratic polynomial. To evaluate the integral in (13), we use a classical composite Gaussian rule with precision degree three, inherited from the one defined in the whole domain.

In case of non-homogeneous Dirichlet boundary conditions, the boundary degrees of freedom, i.e. the control variables associated with basis functions that do not vanish on Γ_D, have to be computed and we have to change the right term in the linear system (9)

(see [5, 7]). The implementation of the Dirichlet boundary conditions is not trivial and it is still a matter of research (see e.g. [4] and the reference therein). In this paper we propose some examples of the above kind, where we choose the control variables associated with basis functions that do not vanish on Γ_D as the solution of a univariate spline interpolation problem.

4 Numerical examples

In this section we propose some numerical examples to show the performance of the bivariate quadratic B-splines on criss-cross triangulations for the solution of Poisson's problems with mixed boundary conditions. We perform h-refinement by adding at every step a middle knot in each interval of the partitions. With the global geometry function defined in (5), we reproduce the physical domain and this initial exact representation is retained during the refinement process.

In each table we give the number of subintervals $m+1$ and $n+1$ in the two directions s and t, respectively and the discrete L^2-norm of the error $(u-u_h)$, computed on a 35×35 grid of evaluation points in Ω_0, denoted by Ψ.

Example 1

Firstly we consider a very simple example, where $\bar{\Omega}\equiv\Omega_0$

$$\begin{cases} -\Delta u = f, & \text{in } (0,1)^2, \\ u = g, & \text{on } x=0,\ y=0 \\ \dfrac{\partial u}{\partial \mathbf{n}} = g_N, & \text{on } x=1, y=1, \end{cases}$$

with f, g and g_N obtained from the exact solution $u(x,y)=3x^2+2y^2$. In order to reproduce the domain, we consider the coarse knot partitions $\bar{\xi}=\bar{\eta}=(0,1)$. Therefore, we have $M=N=3$, $\mathcal{K}_{MN}=\mathcal{K}_{33}=\{(i,j):0\le i,j\le 2\}$ and $\mathbf{G}(s,t)=\sum_{(i,j)\in\mathcal{K}_{33}}\mathbf{P}_{ij}B_{ij}(s,t)$, with $(s,t)\in\Omega_0$. Since $\mathbf{G}$ is the identity map, the control points are the nine points $\mathbf{P}_{ij}=\{(s_i^p,t_j^p),\ 0\le i,j\le 2\}$, defined as in (6). Then, we perform h-refinement, considering $m,n=1$, 3, 7, 15, 31 and smoothness vectors $\bar{\mu}^{\xi}$, $\bar{\mu}^{\eta}$ with elements equal to one. We report the results in Table 1. According to Section 2, we remark that we have to neglect one inner B-spline either with C^1 smoothness everywhere or with C^0 smoothness only on the boundary of its support, in order to obtain a basis.

$m+1=n+1$	2	4	8	16	32
L^2-error	4.0(-15)	2.5(-15)	3.6(-15)	1.3(-15)	1.6(-14)

Table 1: Example 1. Error in L^2-norm versus interval number per side.

 ISBN:978-84-615-5392-1

We can notice that the solution, i.e. a quadratic polynomial, is reproduced. The computation of derivatives and integrals is stable, because there is not deterioration of the approximation error increasing the refinement.

Example 2

In this example we consider the Poisson's problem in the L-shape domain shown in Fig. 1(b)

$$\begin{cases} -\Delta u = f, & \text{in } \Omega, \\ u = 0, & \text{on } \Gamma_D = \partial\Omega, \end{cases}$$

where f is obtained from the exact solution $u(x,y) = \sin(\pi x)\sin(\pi y)$. In order to reproduce the domain, we can use two approaches, as in [11]. To introduce a discontinuity in the first derivative and create the corners, we can place two control points at the same location in physical space or we can use suitable double knots in $\bar{s}$ and $\bar{t}$. In the first case, we ensure that the basis has C^1 continuity throughout the interior of the domain. The only place where the basis is not C^1 is on the boundary itself, at the location of the repeated control points. We consider both cases in order to compare the corresponding results.

Approach 1: Double control point. We start with the coarse knot partitions $\bar{\xi} = (0, \frac{1}{2}, 1)$, $\bar{\eta} = (0,1)$ and we assume $\bar{\mu}^{\bar{\xi}} = (1)$. Therefore, we have $M = 4$, $N = 3$, $\mathcal{K}_{MN} = \mathcal{K}_{43} = \{(i,j) : 0 \le i \le 3,\ 0 \le j \le 2\}$ and $\mathbf{G}(s,t) = \sum_{(i,j)\in\mathcal{K}_{43}} \mathbf{P}_{ij} B_{ij}(s,t)$, with $(s,t) \in \Omega_0$ and the control points given in Fig. 1(c). In Fig. 1(a) we show the parameter domain Ω_0, with the associated knot sequences and, in Fig. 1(b), the corresponding physical domain Ω, with the control points.

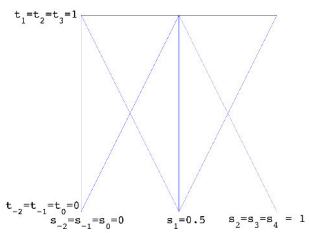

(a)

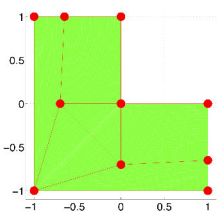

(b)

i	$\mathbf{P}_{i0}$	$\mathbf{P}_{i1}$	$\mathbf{P}_{i2}$
0	$(-1,1)$	$(-0.65,1)$	$(0,1)$
1	$(-1,-1)$	$(-0.7,0)$	$(0,0)$
2	$(-1,-1)$	$(0,-0.7)$	$(0,0)$
3	$(1,-1)$	$(1,-0.65)$	$(1,0)$

(c)

Figure 1: Example 2, Approach 1. (a) Parameter domain Ω_0, (b) physical domain Ω and (c) control points.

Then, we perform h-refinement, considering $m = 1, 3, 7, 15, 31$, $n = 0, 1, 3, 7, 15$, the smoothness vectors $\bar{\mu}^{\xi}$, $\bar{\mu}^{\eta}$ with elements equal to one and we report the results in the second row of Table 2.

In Figs. 2(a)$\div$(c) we give the graphs of the exact solution, the approximation computed with $m = 7$, $n = 3$ and the discrete L^∞-norm error computed on Ψ.

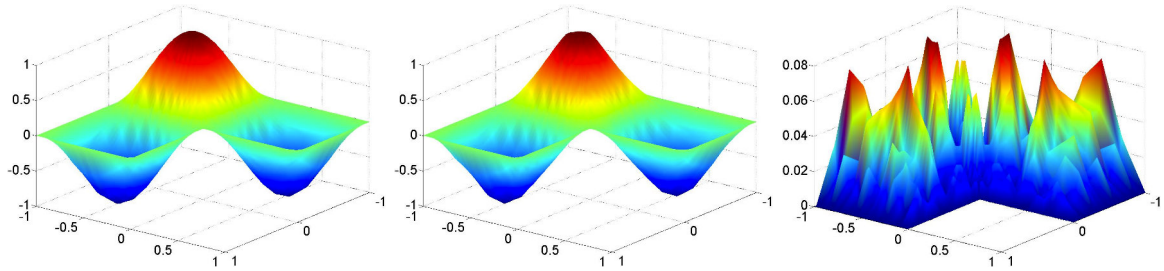

(a) (b) (c)

Figure 2: Example 2, Approach 1. The graphs of (a) the exact solution, (b) the approximation computed with $m = 7$, $n = 3$, (c) the discrete L^∞-norm error computed on Ψ.

Approach 2: Double knot. We start with the coarse knot partitions $\bar{\xi} = (0, \frac{1}{2}, 1)$, $\bar{\eta} = (0, 1)$ and we assume $\bar{\mu}^{\bar{\xi}} = (0)$. Therefore, we have $M = 5$, $N = 3$, $\mathcal{K}_{MN} = \mathcal{K}_{53} = \{(i, j) : 0 \le i \le 4,\ 0 \le j \le 2\}$ and $\mathbf{G}(s, t) = \sum_{(i,j)\in\mathcal{K}_{53}} \mathbf{P}_{ij} B_{ij}(s, t)$, with $(s, t) \in \Omega_0$ and the control points given in Fig. 3(c). In Fig. 3(a) we show the parameter domain Ω_0, with the associated knot sequences and, in Fig. 3(b), the corresponding physical domain Ω, with the control points.

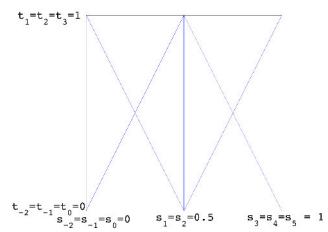

(a)

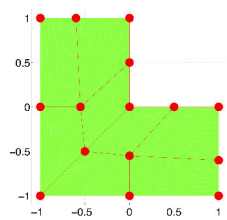

(b)

i	$\mathbf{P}_{i0}$	$\mathbf{P}_{i1}$	$\mathbf{P}_{i2}$
0	$(-1, 1)$	$(-0.6, 1)$	$(0, 1)$
1	$(-1, 0)$	$(-0.55, 0)$	$(0, 0.5)$
2	$(-1, -1)$	$(-0.5, -0.5)$	$(0, 0)$
3	$(0, -1)$	$(0, -0.55)$	$(0.5, 0)$
4	$(1, -1)$	$(1, -0.6)$	$(1, 0)$

(c)

Figure 3: Example 2, Approach 2.(a) Parameter domain Ω_0, (b) physical domain Ω and (c) control points.

Then, we perform the same h-refinement of Approach 1. In this case the smoothness vector $\bar{\mu}^\eta$ has elements equal to one, while $\bar{\mu}^\xi$ has all of the elements equal to one except the element corresponding to $s = \frac{1}{2}$, that is equal to zero. We report the results in the third row of Table 2. In order to obtain a basis, according to Section 2, we remark that we have to neglect two inner B-splines either with C^1 smoothness everywhere or with C^0 smoothness only on the boundary of their support, because in this case the domain Ω is subdivided into two subdomains.

In Figs. $4(a) \div (c)$ we give the graphs of the exact solution, the approximation computed

with $m = 7$, $n = 3$ and the discrete L^∞-norm error computed on Ψ.

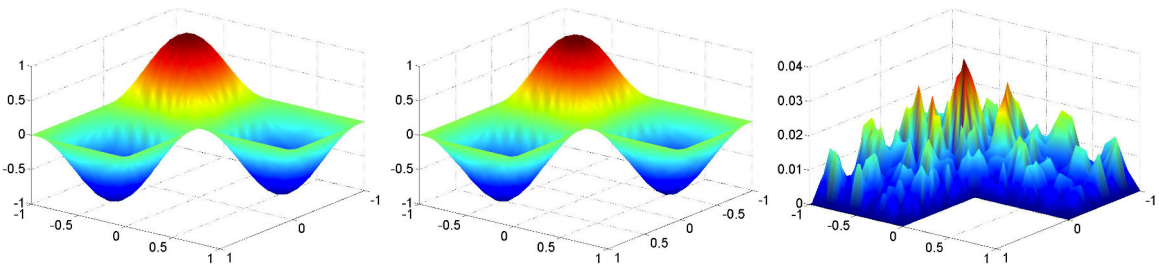

(a) (b) (c)

Figure 4: Example 2, Approach 2. The graphs of (a) the exact solution, (b) the approximation computed with $m = 7$, $n = 3$, (c) the discrete L^∞-norm error computed on Ψ.

$(m+1, n+1)$	(2,1)	(4,2)	(8,4)	(16,8)	(32,16)
L^2-error for Approach 1	7.1(-1)	4.5(-1)	5.3(-2)	6.4(-3)	6.2(-4)
L^2-error for Approach 2	8.3(-1)	2.2(-1)	1.7(-2)	1.6(-3)	1.8(-4)

Table 2: Example 2. Error in L^2-norm versus interval number per side.

In [11] the authors solve the same problem, by considering the two above approaches, but they use a method based on biquadratic tensor product B-splines. If we analyse our results and theirs, we can conclude that the two methods are comparable.

Example 3

In this example we consider the Poisson's problem in the domain shown in Fig. 5(b)

$$\begin{cases} -\Delta u = f, & \text{in } \Omega, \\ u = g, & \text{on } \Gamma_D, \\ \dfrac{\partial u}{\partial \mathbf{n}} = g_N, & \text{on } \Gamma_N, \end{cases}$$

where Γ_N is given by the two segments with endpoints (-4,0), (0,0) and (-2,4), (2,4), respectively and Γ_D is given by the two parabolic sections with endpoints (-4,0), (-2,4) and (0,0), (2,4). The functions f, g and g_N are obtained from the exact solution $u(x, y) = \frac{\sin(x^2+y^2-1)}{5}$. In order to reproduce the domain, we consider the coarse knot partitions $\bar{\xi} = \bar{\eta} = (0, 1)$. Therefore, we have $M = 3$, $N = 3$, $\mathcal{K}_{MN} = \mathcal{K}_{33} = \{(i, j) : 0 \leq i, j \leq 2, \}$ and $\mathbf{G}(s, t) = \sum_{(i,j)\in\mathcal{K}_{33}} \mathbf{P}_{ij} B_{ij}(s, t)$, with $(s, t) \in \Omega_0$ and the control points given in Fig. 5(c). In Fig. 5(a) we show the parameter domain Ω_0, with the associated knot sequences and, in Fig. 5(b), the corresponding physical domain Ω, with the control points.

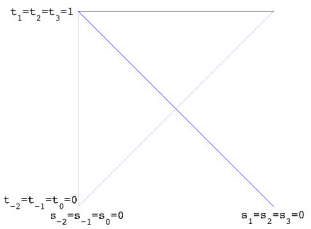

(a)

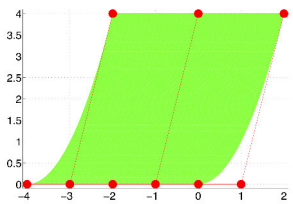

(b)

i	$\mathbf{P}_{i0}$	$\mathbf{P}_{i1}$	$\mathbf{P}_{i2}$
0	$(-4,0)$	$(-3,0)$	$(-2,4)$
1	$(-2,0)$	$(-1,0)$	$(0,4)$
2	$(0,0)$	$(-1,0)$	$(2,4)$

(c)

Figure 5: Example 3.(a) Parameter domain Ω_0, (b) physical domain Ω and (c) control points.

Then, we perform h-refinement, considering $m, n = 1,\ 3,\ 7,\ 15,\ 31$ and, in Table 3, we report the results. In Figs. $6(a) \div (c)$ we give the graphs of the exact solution, the approximation computed with $m = n = 7$ and the discrete L^∞-norm error computed on Ψ.

$m+1 = n+1$	2	4	8	16	32
L^2-error for Case 1	9.9(-1)	1.3(-1)	3.4(-2)	4.3(-3)	4.5(-4)

Table 3: Example 3. Error in L^2-norm versus interval number per side.

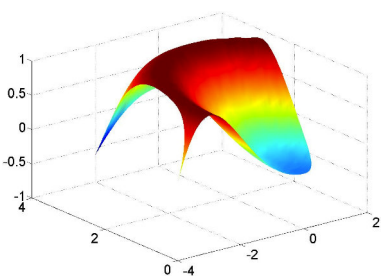

(a)

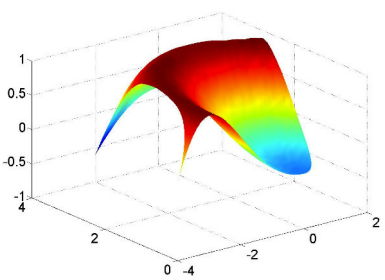

(b)

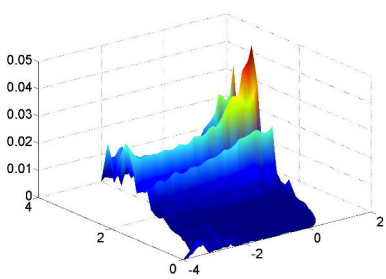

(c)

Figure 6: Example 3. The graphs of (a) the exact solution, (b) the approximation computed with $m = n = 7$, (c) the discrete L^∞-norm error computed on Ψ.

References

[1] P. Costantini, C. Manni, F. Pelosi, M. L. Sampoli, *Quasi-interpolation in isogeometric analysis based on generalized B-splines*, Comput. Aided Geom. Design **27** (2010) 656–668.

[2] C. Dagnino, P. Lamberti, S. Remogna, *BB-coefficients of unequally smooth quadratic B-splines on non uniform criss-cross triangulations*, Quaderni Scientifici del Dipartimento di Matematica, Università di Torino, **24** (2008) http://hdl.handle.net/2318/434

[3] C. Dagnino, P. Lamberti, S. Remogna, *On unequally smooth bivariate quadratic spline spaces*, Computational and Mathematical Methods in Science and Engineering (J. Vigo Aguiar Ed.), (2009) 350–359.

[4] C. de Falco, A. Reali, R. Vázquez, *GeoPDEs: a research tool for Isogeometric Analysis of PDEs*, Adv. Eng. Softw. **42** (2011) 1020–1034.

[5] T. J. R. Hughes, J. A. Cottrell, Y. Bazilevs, *Isogeometric Analysis. Toward integration of CAD and FEA*, WILEY, 2009.

[6] J. N. Lyness, R. Cools, *A Survey of Numerical Cubature over Triangles*, Mathematics and Computer Science Division, Argonne National Laboratory **III** 1994.

[7] A. Quarteroni, *Numerical Models for Differential Problems, Modeling, Simulation & Applications*, Springer, 2009.

[8] P. Sablonnière, *Quadratic B-splines on non-uniform criss-cross triangulations of bounded rectangular domains of the plane*, Report IRMAR **03-14**, University of Rennes (2003)

[9] P. Sablonnière, *Quadratic spline quasi-interpolants on bounded domains of* $\mathbb{R}^d, d = 1, 2, 3$, Rend. Sem. Mat. Univ. Pol. Torino **61** (2003) 229–238.

[10] H. Speleers, C. Manni, F. Pelosi, M. L. Sampoli, *Isogeometric analysis with Powell-Sabin splines for advection-diffusion-reaction problems*, Comput. Methods Appl. Mech. Engrg. **221-222** (2012) 132–148.

[11] A. V. Vuong, Ch. Heinrich, B. Simeon, *ISOGAT: a 2D tutorial MATLAB code for Isogeometric Analysis*, Comput. Aided Geom. Design **27** (2010) 644–655.

[12] R. H. Wang, *Multivariate Spline Functions and Their Application*, Science Press, Beijing/New York, Kluwer Academic Publishers, Dordrecht/Boston/London, 2001.

[13] R. H. Wang C. J. Li, *A kind of multivariate NURBS surfaces*, J. Comp. Math. **22** (2004) 137–144.

[14] G. von Winckel, *Matlab procedure* `triquad`, http://www.mathworks.com/matlabcentral/fileexchange/9230-gaussian-quadrature-for-triangles.